

Electrochemistry of Conductive Polymers 37. Nanoscale Monitoring of Electrical Properties during Electrochemical Growth of Polypyrrole and Its Aging

Hyo Joong Lee and Su-Moon Park*

Department of Chemistry and Center for Integrated Molecular Systems, Pohang University of Science and Technology, San 31, Hyoja-dong, Pohang, Gyeongbuk 790-784, Korea (Republic of Korea)

Received: February 11, 2005; In Final Form: May 16, 2005

Electrical and morphological properties of polypyrrole (PPy) films were studied during and after their electrochemical growth under various experimental conditions on a nanometer scale using a current-sensing atomic force microscope (CS-AFM). Of acetonitrile (ACN) solutions containing various amounts of water, one that contained 1.0% water produced the best quality films in their electrical and morphological properties in terms of homogeneities. The degree of doping, as well as time evolution of the film structure and its conductivity, of the PPy films was investigated during their growth in water and ACN with 1.0% water by obtaining the current images at a few designated growing stages, and the results were compared. Well-doped, conductive films were obtained from the very early stage during the electrodeposition of PPy in the ACN solution, while the films were poorly doped in water. As the film deposition progressed further in both aqueous and nonaqueous media, the doped areas spread over the whole surface leading to a more homogeneously conducting film. The current–voltage traces were obtained at each growing stage, which showed that the conductivity increases in both media as the PPy grows; the conductivity of the film grown in ACN is much higher than that of the film grown in water at all growing stages. The electrical properties of the PPy film deteriorated gradually upon exposure to air.

Introduction

Recently, studies of electron transport properties of organic single molecules,¹ oligomers,² polymers,³ and other nanostructures⁴ have been carried out successfully using an AFM technique with a conducting tip. These studies have revealed that the AFM technique is a very powerful tool and essential in investigating the nano or molecular scale electronic transport properties as well as spatial distributions of conducting areas.

Polypyrrole (PPy) is one of the most studied conducting polymers because of its rather straightforward preparation and reasonable stabilities in air and in aqueous media. In addition, electrodeposited PPy films have a well-defined grain structure and a relatively smooth surface.^{3b,5} Thus, PPy can be a good model system in studying the effects of various experimental conditions on the properties of the resulting film. There have been many studies reported on the effects of experimental conditions on the electropolymerization processes.⁶ However, most of the studies published thus far on the electrochemical preparation of conducting polymers have addressed problems related to their chemical as well as electrochemical properties,⁷ growth kinetics,⁸ and mechanisms;⁹ not much attention has been paid to morphological and conducting properties of these polymers during their growth. This was primarily due to the difficulty encountered in monitoring both the morphology and the conductance during the growth even if the measurements had to be made *ex situ*. The resulting morphological features of the polymer films could be studied by scanning electron microscopy¹⁰ (SEM) or scanning tunneling microscopy¹¹ (STM) in very limited cases. To characterize electrical properties of polymer films, investigators usually measured bulk conductivi-

ties by a four probe method,¹² but it would be difficult to collect the sample enough to measure the bulk conductivity at an early stage of electrochemical preparation. For this reason, reports on changes in the morphology and conductance monitored during the polymer growth are sparse if they do exist.

In this study, we demonstrate by using a current-sensing AFM that changes in both the morphology and the conductance can be monitored in nanoscale during the electrochemical growth of an organic film. The results show from the two-dimensional current images that a small change in water content of an organic solvent, as well as the solvent itself, can drastically affect the electrical properties of electrodeposited PPy films.

Experimental Section

Acetonitrile (ACN: Aldrich 99.8%, anhydrous) was used as received. Lithium perchlorate (LiClO₄, Aldrich 99.99%) was used after drying in a vacuum oven at 110 °C for 16 h. Pyrrole (Aldrich, 98%) was used after distillation over zinc powder and stored in the dark under a nitrogen atmosphere. An electrochemical cell with a three-electrode configuration was used for electrochemical experiments. A gold-on-silicon electrode (with Cr adhesive layers, LGA films) was annealed by a hydrogen flame and used as a working electrode (active area: 0.255 cm²). A platinum gauze and a silver wire dipped in a 0.10 M AgNO₃ solution in ACN in a separate compartment were used as counter and reference electrodes, respectively. In aqueous media, an Ag/AgCl (in saturated KCl) electrode was used as a reference electrode instead. PPy films were grown galvanostatically by applying 1.0 mA (3.92 mA/cm²) for 10 s, or 0.40 mA (1.57 mA/cm²) for certain designated time, using an EG&G model 273 potentiostat-galvanostat after purging with N₂ for 30 min through a water or an ACN solution containing 0–2% water,

* Corresponding author. E-mail: smpark@postech.edu. Phone: +82-54-279-2102. Fax: +82-54-279-3399.

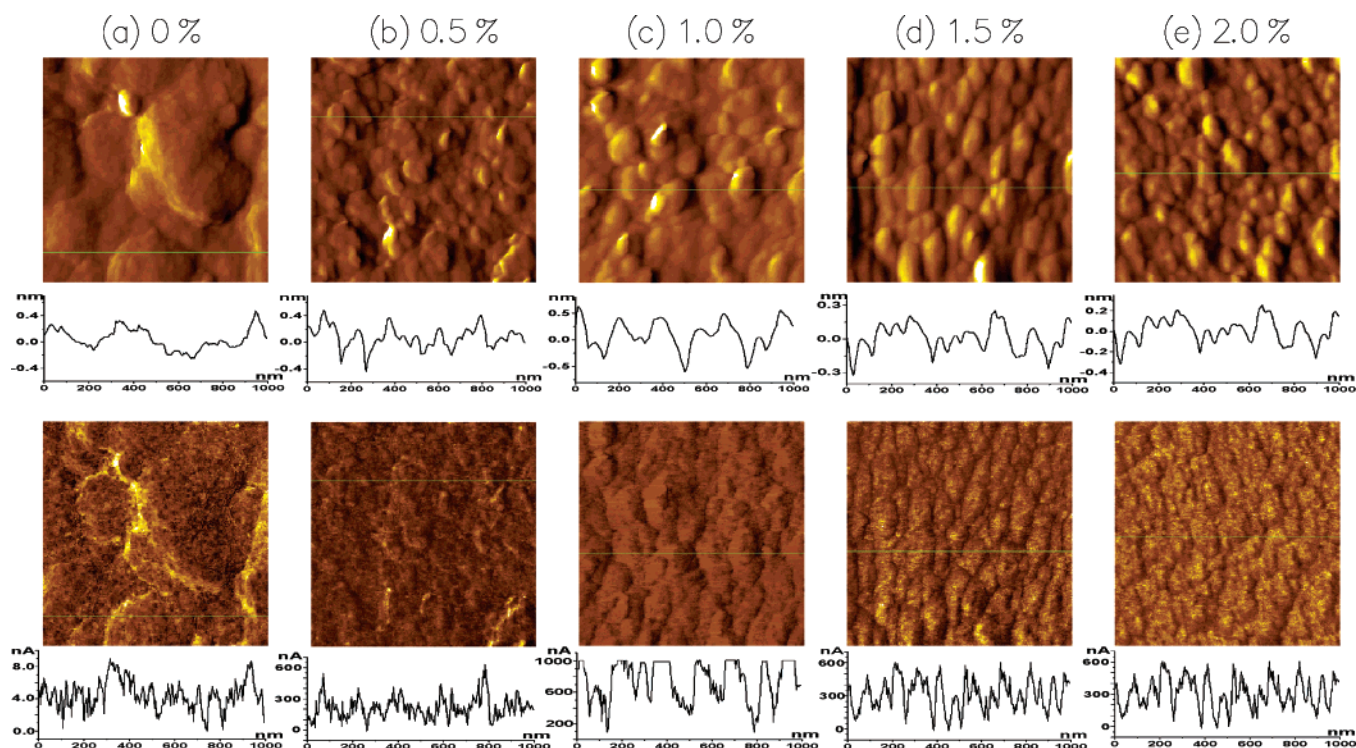


Figure 1. Simultaneously recorded deflection (top) and current (bottom) images of as-grown PPy films from ACN with the water content indicated and their cross sectional analyses. The bias voltage between the substrate gold electrode and the tip was 5.0 mV and the scan area was $1 \times 1 \mu\text{m}$.

0.10 M pyrrole, and 0.10 M LiClO_4 . After the electrochemical synthesis, the films were rinsed with pure water or ACN and dried in a vacuum at room temperature. The films prepared in ACN and in water by passing an identical anodic charge of 39.2 mC/cm^2 had thicknesses of 110 and 125 nm, respectively, from the cross-sectional views of their SEM images; these agree well with a reported value that 379 mC corresponds approximately to $1.0 \mu\text{m}$.¹³

The contact mode AFM with a current-sensing module, so-called current sensing AFM (PicoSPM, Molecular Imaging Inc.)¹⁴ was used to simultaneously obtain topographical (or deflection) and current images. The platinum–iridium (PtIr) coated cantilevers (spring constant, 0.25 N/m) were purchased from Nanosensors. The load force was maintained at 6 nN to avoid the damage of the tip and the sample. A bias voltage between the substrate (Au) and the conducting cantilever, which is grounded, was 5 or 50 mV during the imaging experiments. Before imaging the PPy films, the surface was purged by the high purity N_2 gas to minimize the effects of moisture, and all the AFM experiments were carried out in this controlled environment. The topographical and current images recorded before, during, and after the point contact, and current–voltage (I–V) measurements were identical as long as the load force was maintained below 10 nN, indicating that the tips and the samples are not damaged easily during the measurements. The data were discarded and tips exchanged whenever the images were different before, during, or after a series of electrical measurements.

The UV–vis absorption spectra of PPy films on the gold-on-silicon electrode were taken with an Oriel InstaSpec IV spectrometer with a charge coupled device (CCD) array detector, which was configured in a near normal incidence reflectance mode using a bifurcated quartz optical fiber.^{3d,15} The reference spectrum was first taken from a clean bare gold-on-silicon electrode. A dried PPy-covered electrode was then placed at the end of the bifurcated optical fiber instead of the bare gold-

on-silicon electrode and the absorption spectrum of the film was recorded.

Results and Discussion

To find optimal experimental conditions leading to the best quality PPy films, we first ran experiments in ACN containing 0.10 M pyrrole, 0.10 M LiClO_4 , and a given amount of water, which varied from 0% to 2.0% in a 0.50% increment. It has been well-known from purely an empirical point of view, from when the first PPy preparation was reported,¹⁶ that a small amount of water (1–2%) should be added to effectively electropolymerize pyrrole in the ACN medium. However, a few investigators claim that addition of 1.0% of water yields the best quality PPy film while others still used an acetonitrile solution with 2.0% water in preparing PPy films.^{10b,c,16} In efforts to evaluate films thus prepared, the bulk conductivities and charge storage capacities of the films were compared after they were prepared with different amounts of water present in ACN because these properties could be the indicators for how good the films were.^{16a,d} In our study, we were able to straightforwardly monitor the effects of the small amounts of water on electrical properties of the resulting films by obtaining 2-D topographical and current images. Figure 1 shows a series of deflection and current images simultaneously obtained from the PPy films galvanostatically grown in ACN with a different water content (0–2%) under otherwise an identical experimental condition. As we prepared these PPy films under the same experimental conditions in ACN with a different amount of water and both topographical and current images were obtained at an identical bias voltage of 5 mV with an identical loading force (6 nN), we can see the effects of the water content on the morphological and conductive properties of the film on a nanometer scale by simply comparing the images.

In the case of ACN with no water added (Figure 1a), a higher overpotential by approximately 0.20 V was measured in

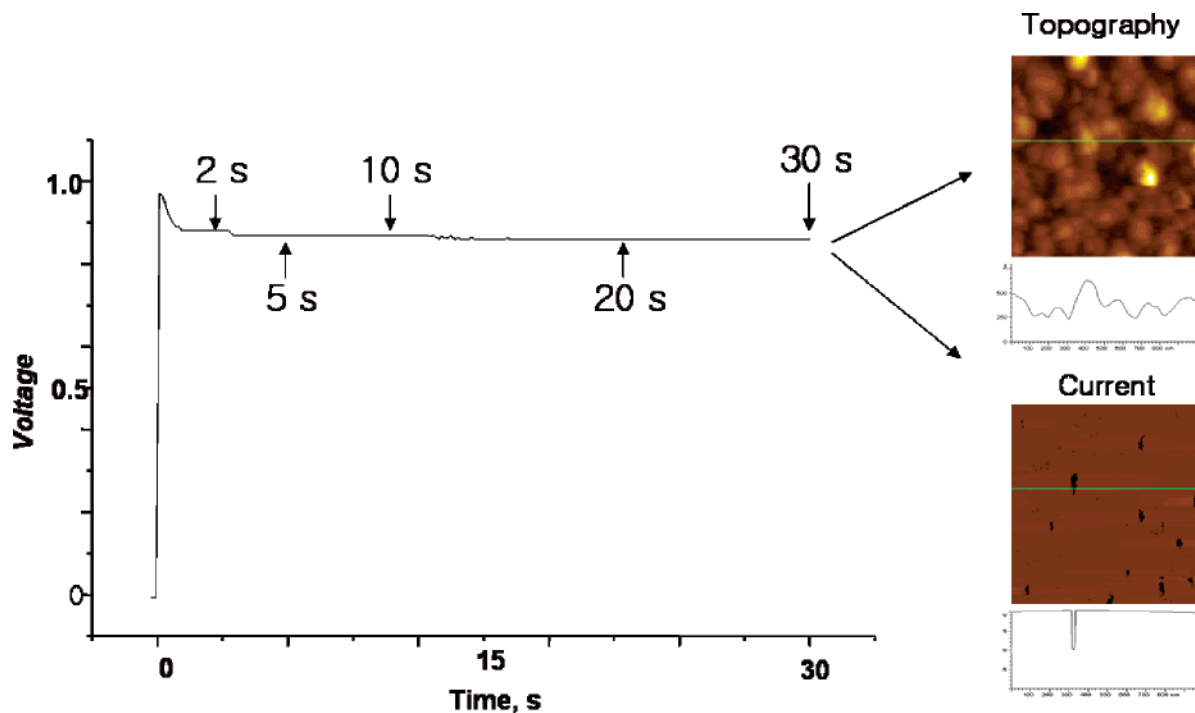


Figure 2. Schematic diagram for obtaining topographic and current images at each designated growing stage.

comparison to those in ACN solutions containing water, even when an identical anodic current (39.2 mA/cm^2) was passed at the working electrode during its preparation in comparison to other four cases. This could very well be due to the increased resistances of the solution and the polymer film, as well as the charge transfer reaction. The film obtained thereof also recorded a very low average current of 4.3 nA over the scanned area at a bias voltage of 5 mV (Figure 1a, bottom), which attests that the film thus obtained is significantly more resistive than those prepared in ACN containing water; the average currents were obtained by averaging the currents across the cross-sectional line shown below the current image. These observations indicate that the ACN system with no water is not as effective in electropolymerizing pyrrole as the ACN system containing a small amount of water, as can be seen from the much lower current scale used for the current profile (Figure 1a); mechanisms have been proposed for the role of water molecules during the electrochemical polymerization of pyrrole.^{16b,c,17} The morphology obtained from the ACN system with no water was also very different from the other four cases. Large hilly domains, as well as lower valleys, of as wide as a few hundred nm are observed over on the film surface while the surfaces of polymers prepared with water present are made of relatively regular and smaller grains.

As can be seen from the cross sectional analysis of current images, the most conductive film was obtained from the ACN solution containing 1.0% water; the conductivity of the film as seen from the current profiles shown below the current images then decreased in the order of the films prepared with the water content of $1.5\% \approx 2.0\% > 0.50\% \gg 0\%$. For the PPy film obtained from the 1.0% water-ACN solution, the currents recorded from the surface through the film are more homogeneous than through any other films and reach a saturation value of $1 \mu\text{A}$ at a small bias voltage (5 mV), which corresponds to a highly conducting metallic state (Figure 1c). When the scanned area was expanded from $1 \mu\text{m} \times 1 \mu\text{m}$ to $10 \mu\text{m} \times 10 \mu\text{m}$, the surface looked almost perfectly uniform (images not shown); the differences could not be seen in nanoscale when the larger areas are scanned. Also, it is seen fairly clearly in this

experiment that the tops of grains are generally more conducting than the valleys. This is perhaps due to the fact that the top region is more easily oxidized (doped) and, thus, more conductive, which is consistent with the results obtained using the Kelvin probe method¹⁸ as well as in our previous work.^{3b} This observation also indicates that electrical properties are rather inhomogeneous when viewed in nanoscale and different from spot to spot, depending on the morphological features although their averaged values are almost the same. From the magnitude of the average currents at the indicated lines below the current images, the films obtained from the 1.5% and 2.0% water-containing systems (Figure 1 d,e) exhibit similar electrical properties. For the thicker films of $3\text{--}5 \mu\text{m}$, it was not as straightforward to reach a clear conclusion on the film qualities in terms of their electrical properties as for the thin films because the films were not as homogeneous in both their morphologies and current images. This must be because the thick films are not as well packed as for the thin films. For this reason, the studies on the bulk properties could be more reliable for thick films,¹⁷ in which four-probe methods are used for the samples prepared by pressure compaction.

Having determined the experimental condition to prepare the best quality film in ACN, we then proceeded to monitor the growth characteristics as a function of time in two different solvents, ACN with 1.0% water and pure water. Thus, we ran a series of experiments to see a more detailed time evolution of electrical properties, in which the film growth was stopped at a certain designated growth period (Figure 2), the resulting film was dried, and 2-D topographical and current images were obtained thereof. The PPy films were grown galvanostatically in either H_2O (Figure 3) or ACN containing 1.0% water (Figure 4) by passing a constant current of $400 \mu\text{A}$ (1.57 mA/cm^2); the current density used here was 40% of that used for the films shown in Figure 1 in order to slow the deposition kinetics so that the early deposition process could be seen before a significant amount of the film was accumulated. The topographic (top) and current (bottom) images of the PPy film at different growth periods in water and ACN are shown in Figures 3 and 4, respectively.

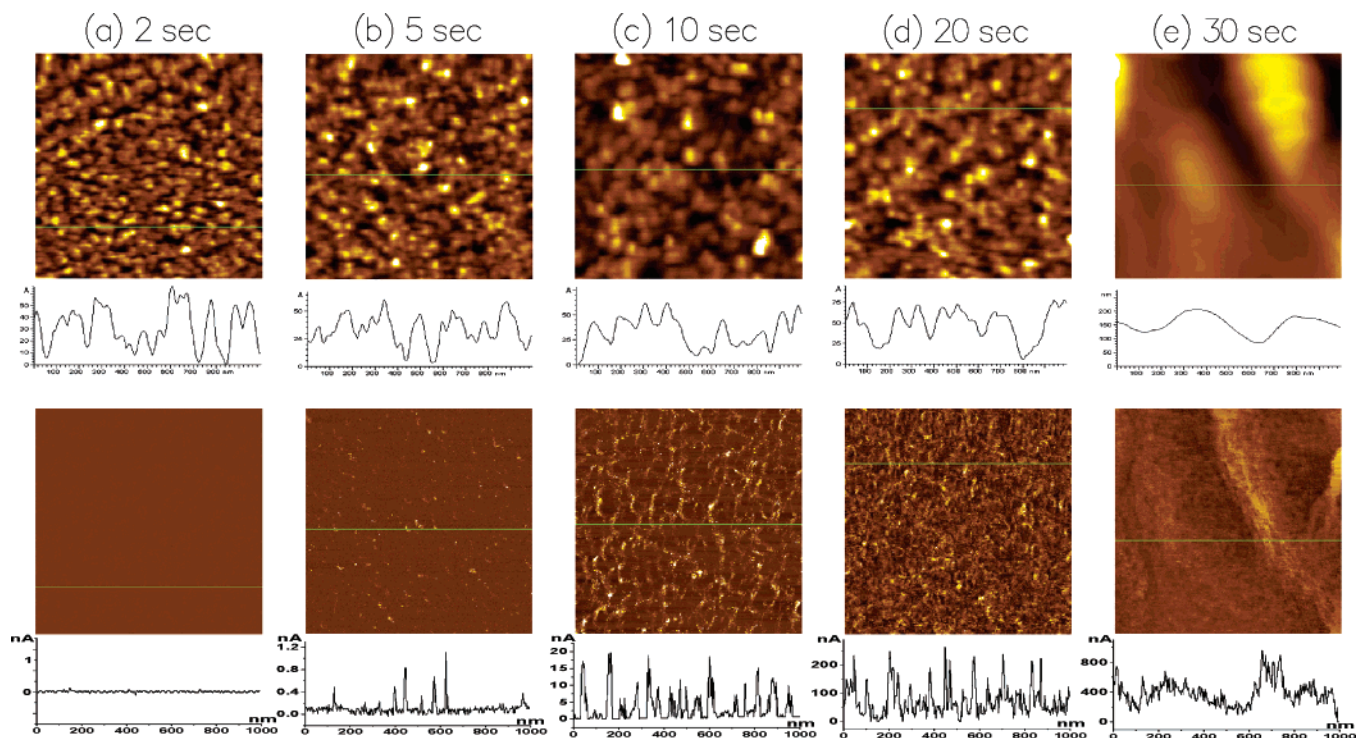


Figure 3. Topographic (top) and current (bottom) images obtained at each growing stage as indicated in Figure 2 for the film prepared in the aqueous medium.

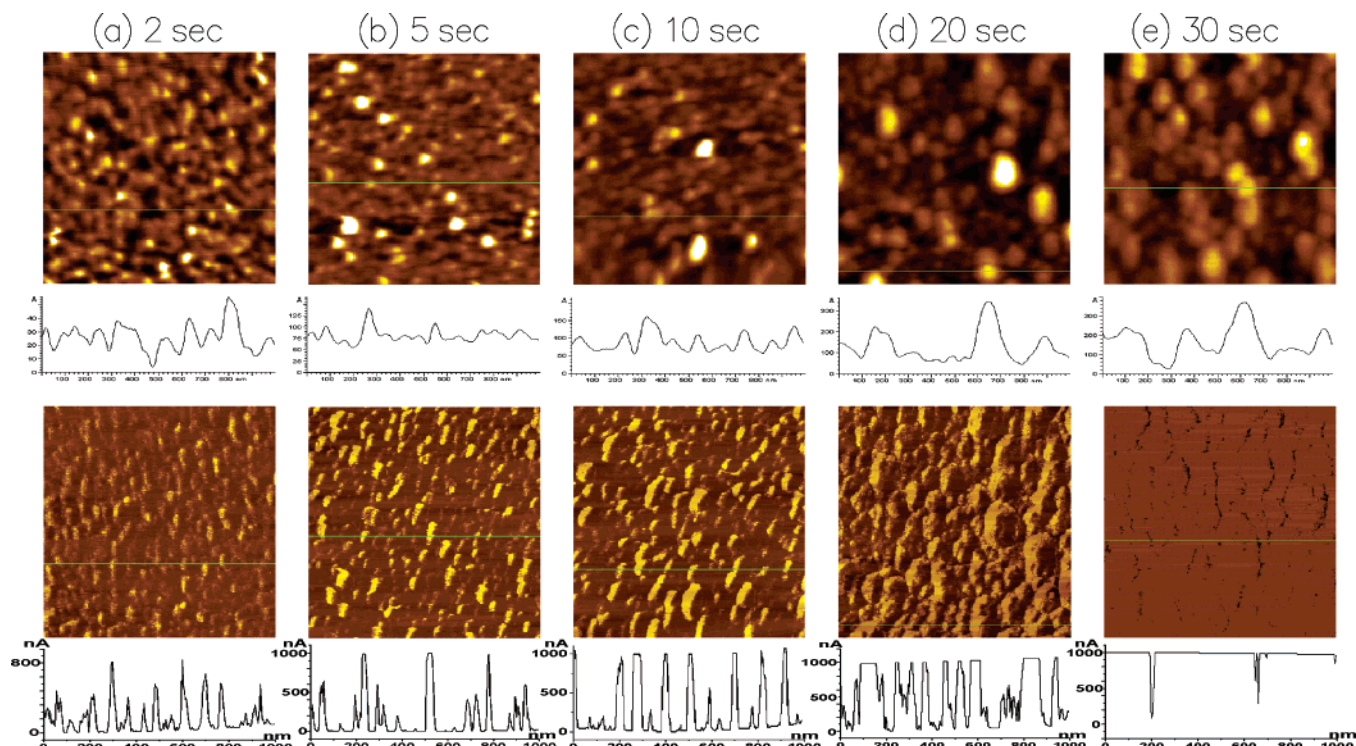


Figure 4. Topographic (top) and current (bottom) images obtained at each growing stage for the film prepared in the 1% water-ACN medium.

At the very early stage of the film growth (2.0 s = 3.14 mC/cm², ~10 nm thick) in water, the surface of the gold-on-silicon electrode seems to have been almost fully covered with a nonconducting thin layer judging from the current image (Figure 3a). However, the current–voltage behavior shown in Figure 5a for this film indicates that it is more semiconducting than

nonconducting. Thus, the electrode is probably covered with undoped or poorly doped short chained PPy and/or pyrrole oligomers at this stage, which are usually observed during the PPy synthesis.¹⁹ Note also that small grains with their diameters of about a few tens of nm appear to be segregated from each other until the film is fully grown (Figure 3e). This observation

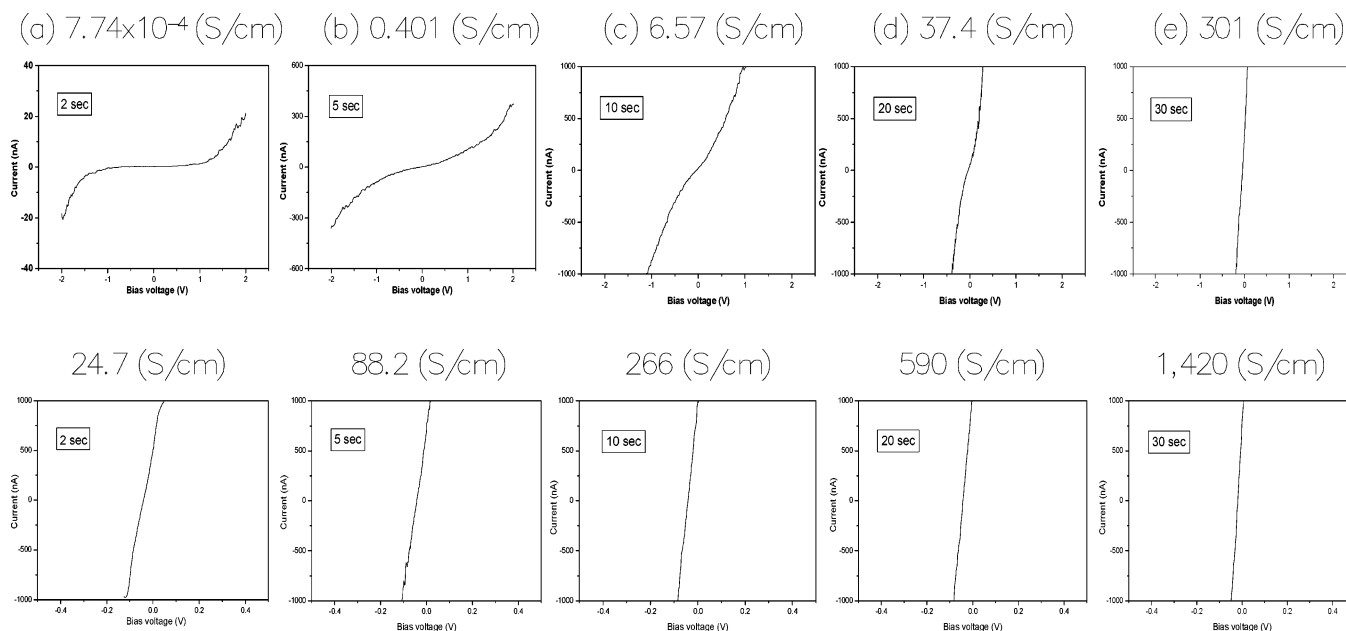


Figure 5. Current-voltage traces recorded during the film growth at more conducting spots in the current images shown in Figure 3 (films prepared in the aqueous medium) and Figure 4 (films prepared in ACN) and their conductivity values.

illustrates that the electrochemical deposition of PPy or pyrrole oligomers and their subsequent doping are very inefficient in water in such a short time. At 5.0 s (7.85 mC/cm², Figure 3b), a few bright spots corresponding to regions of a few nA, which represent a little more conducting areas than most of background spots, appear randomly over the scanned area. The doping process is just beginning at this stage while the film is being formed. When more anodic charges ranging from 15.7 mC/cm² (10 s) to 31.4 mC/cm² (20 s) are used, the grain sizes increase further in topography and current-flowing regions spread over the whole surface as can be seen in Figure 3c,d. Now, the deposition and doping processes seem to have become competitive. As more charge is spent for a longer time (30 s, 47.1 mC/cm²), small grains formed at earlier stages merge into large mountains and valleys with the film becoming more conducting than before. When grown in water, the PPy films always had a similar morphology to the one shown in Figure 3e; the grains had widths of a few hundred nm and heights of a few tens of nm. Also, the current images were rather inhomogeneous with their magnitudes very low in comparison to those of the films prepared in ACN containing 1.0% of water. Finally, it is more difficult to deduce the conductivity of the film at a given spot from topography alone because the topographically higher parts (mountains) do not always represent the areas of higher conductivities (Figure 3e), in contrast to the films prepared in ACN (vide infra). This suggests that the intermediate species such as radical cations generated in water might have undergone side reactions with water to produce a variety of organic functionalities,²⁰ which lower the conductivities.

A large number of bright spots corresponding to relatively high conducting regions were detected in the current image of the PPy film from the very beginning of its electrochemical preparation in the 1.0% water-ACN medium (2.0 s, Figure 4a). Further, the topographically protruding areas are also more conducting in comparison to the lower lying valleys. This indicates that both the deposition and doping processes occur simultaneously even in this early stage, while the processes are inefficient in water with the side reactions suppressing the doping process during this early period. When more anodic

charge is used at 5.0–20 s (Figure 4 b–d), the number of initial bright spots increases and the whole surface becomes covered by them. At 30 s, nearly the whole film surface displays the saturated current except for a few spots (Figure 4e).

Figure 5 shows a set of current-voltage traces obtained at more conducting spots of the films during their growth in water (top) and in the ACN solution with 1.0% water (bottom). To convert the current data into the vertical conductivity through each PPy film, we need the film thickness, l , and the contact area, A , of the probing tip with the film as the conductivity κ has an expression

$$\kappa = \left(\frac{1}{R}\right) \cdot \frac{l}{A}$$

where R is the vertical resistance obtained for the film between the gold substrate and the tip via current measurement. The film thicknesses were measured from the cross-sectional views of the SEM images for thick films (≥ 50 nm); thicknesses for thinner films than 50 nm were calculated from the amount of charge passed. The contact area of the probe with the film was calculated using the Hertz theory.²¹ As can be seen from the current-voltage curves shown in Figure 5, the conductivity increases as the deposition proceeds in both solvents, and the conductivities of the films prepared in the ACN solution are always much higher than those observed from films prepared in water for the same amount of charge spent for polymerization. In the case of the film prepared in water, the conductivity of the film starts from a lightly doped semiconducting (2.0 s: 7.7×10^{-4} S/cm) through a moderately doped (5.0 s: 0.40 and 10 s: 6.6 S/cm) and a highly doped (20 s: 37.4 S/cm), eventually to nearly a metallic state (30 s: 120 S/cm).^{3d} However, the film grown in ACN (with 1.0% water) shows bright spots with a highly doped semiconducting state from the very early deposition stage (2.0 s: 24.7 S/cm and 5.0 s: 88.2 S/cm), which becomes a metallic state just from 10 s (10 s: 266, 20 s: 590, and 30 s: 1,420 S/cm). Note that the film grown for 2.0 s in ACN has almost the same conductivity as that grown for 20 s in water. This set of the data illustrates quantitatively how the

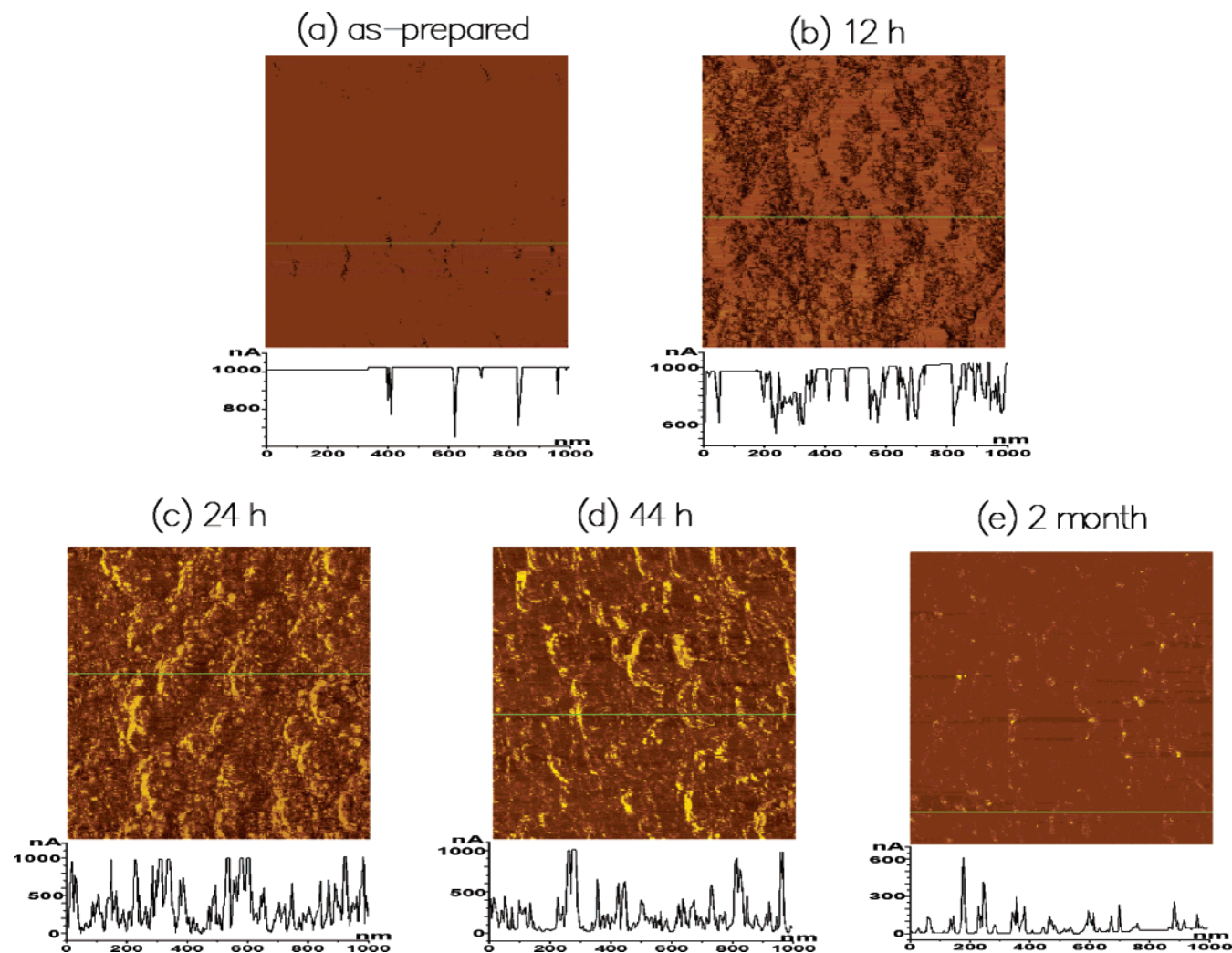


Figure 6. Current images for the PPy film recorded after each designated time has elapsed.

different solvents affect the electrical characteristics of a conducting polymer film and how conductive films emerge from the early stage of growth in a given solvent.

For the π -conjugated (conducting) polymers prepared for use in organic electronics²² or for any other purposes, their stability is a very important factor even after their performance has been demonstrated. Thus far, the stability of the conducting polymers has been evaluated in solution under rather harsh reaction conditions.^{20,23} This is because there was no better way of characterizing the stability of these polymers than those experiments. Organic devices have been found relatively unstable in air in comparison to their inorganic counterparts due to oxidation and degradation processes in the ambient atmosphere,²⁴ and obviously the results of degradation reactions run under the harsh experimental conditions would not be directly applicable to the prediction of the stabilities of these materials in organic devices. Here we examine the time evolution of the current image and the absorption spectrum of the PPy film, which was prepared under the condition (1.0% water in ACN) to produce the best quality, as a function of aging time employing CS-AFM and reflectance spectroscopic techniques.

The five current images shown in Figure 6 represent a typical time evolution of the current flowing over the substrate surface through the PPy film to the tip when it was exposed to dry air. The as-prepared PPy film showed very high conducting characteristics (Figure 6a). The current tops a full scale value

of 1 μ A at a bias voltage of 50 mV over the whole film except at a few spots when the film was freshly prepared, washed, and dried. The current image shown in Figure 6b was obtained after the sample had been left exposed to air in a desiccator for 12 h. Now, the regions of the saturated current slightly diminished starting from the boundary region of well defined grains. After 24 h, the saturated currents were detected only at a few spots with most of the surface rather poorly conducting as can be seen in Figure 6c. Figure 6d shows the current image scanned after 44 h later. The conductance of the sample is entirely different from what we had for the freshly prepared sample.

When the absorption spectrum was taken after the film had been aged for 44 h and compared with that of the as prepared film (Figure 7), the polaron peak representing the degree of doping or the conductivity still remains dominant in the spectrum although the band became broader and its intensity decreased by about 23%. Thus, the large decrease in the average current by about 69%, as shown in Figure 6d mostly appears to arise from the surface degradation due to the reactions with oxygen and water vapor present in the ambient atmosphere.²⁵ As we have noted earlier, the conductivity decreases exponentially for a linear decrease in absorbance.^{3d} The degradation reaction on the surface appears to result in the formation of a thin insulating layer and raise the barrier height of electron transport, leading to a large decrease in the current flowing over the film surface. Also, the degradation product(s) should be

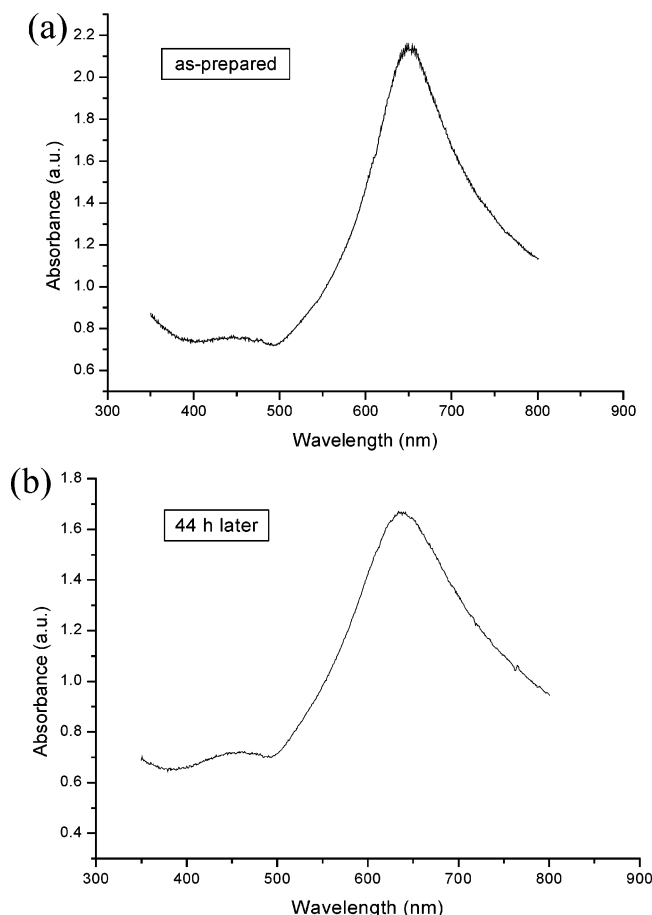


Figure 7. (a) Absorption spectrum taken immediately after the film was prepared (Figure 6a), and (b) the spectrum taken after the film was exposed to air for 44 h (Figure 6d).

responsible for the band broadening of the spectrum. The degradation products of PPy were shown to contain carbonyl groups, which eventually degrades to fumaric acid.^{20b,c} The film becomes almost an insulator in two months as shown in Figure 6e.

Conclusion

We have demonstrated in this study that various electrical properties and their changes of PPy films electrodeposited could be mapped on a nanometer scale employing the CS-AFM technique, which allows the growth and degradation of conducting polymer films to be monitored. Adding a small amount of water to ACN greatly affected the electrical properties of the resulting PPy films, and the changes in currents flowing over their surfaces were mapped directly in two dimension. The results indicate that ACN containing 1.0% (0.56 M) of water is an optimum solvent for producing the most conducting PPy film under the experimental conditions used in our present work. We have also observed that the PPy films exposed to air degraded slowly and the current decreased over the whole surface area as a function of time. Thus, when we measure and compare the electrical properties of two different organic films, the degradation effect should be taken into account. From the current images and current–voltage characteristics obtained at each growing stage, we were able to monitor how the films were transformed into their conductive states and also how the solvents as well as other parameters affected electropolymerization of a conducting polymer. Our results indicate that the PPy growth and doping progressed more homogeneously and efficiently in the ACN medium containing 1.0% water.

To our knowledge, this is the first time that the conductivity and morphology of a conducting polymer film have been monitored during its growth and degradation. We should also be able to study the electrical and morphological properties as well as their changes for other interesting organic films on the nanometer scale by employing the CS-AFM technique as in this report, which would have been very difficult with any other techniques if not impossible.

Acknowledgment. This work was supported by the Korea Science and Engineering Foundation through the Center for Integrated Molecular Systems at POSTECH, the BK21 Program of the Korea Research Foundation, and the National R&D Project for Nano Science and Technology of the Ministry of Science and Technology of Korea.

References and Notes

- (1) (a) Cui, X. D.; Primak, A.; Zarate, X.; Tomfohr, J.; Sankey, O. F.; Moore, A. L.; Moore, T. A.; Gust, D.; G., H.; Lindsay, S. M. *Science* **2001**, *294*, 571. (b) Leatherman, G.; Durantini, E. N.; Gust, D.; Moore, T. A.; Moore, A. L.; Stone, S.; Zhou, Z.; Rez, P.; Liu, Y. Z.; Lindsay, S. M. *J. Phys. Chem. B* **1999**, *103*, 4006. (c) Rawlett, A. M.; Hopson, T. J.; Nagahara, L. A.; Tsui, R. K.; Ramachandran, G. K.; Lindsay, S. M. *Appl. Phys. Lett.* **2002**, *81*, 3043.
- (2) (a) Loiacono, M. J.; Granstrom, E. L.; Frisbie, C. D. *J. Phys. Chem. B* **1998**, *102*, 1679.
- (3) (a) Zhao, J.; Davis, J. J.; Sansom, M. S. P.; Hung, A. *J. Am. Chem. Soc.* **2004**, *126*, 5601. (b) Lee, H. J.; Park, S.-M. *J. Phys. Chem. B* **2004**, *108*, 1590. (c) Han, D.-H.; Park, S.-M. *J. Phys. Chem. B* **2004**, *108*, 13921. (d) Lee, H. J.; Park, S.-M. *J. Phys. Chem. B* **2004**, *108*, 16365. (e) Ionescu-Zanetti, C.; Mechler, A.; Carter, S. A.; Lal, R. *Adv. Mater.* **2004**, *16*, 385. (f) Hong, S.-Y.; Park, S.-M. *J. Phys. Chem. B* **2005**, *109*, 9305.
- (4) (a) Park, W. I.; Yi, G.-C.; Kim, J.-W.; Park, S.-M. *Appl. Phys. Lett.* **2003**, *82*, 4358. (b) Saha, S. K.; Su, Y. K.; Lin, C. L.; Jaw, D. W. *Nanotechnology* **2004**, *15*, 66. (c) Park, J. G.; Lee, S. H.; Kim, B.; Park, Y. W. *Appl. Phys. Lett.* **2002**, *81*, 4625. (d) Alpers, B.; Cohen, S.; Rubinstein, I.; Hodes, G. *Phys. Rev. B* **1995**, *52*, R17017. (e) Dai, H.; Wong, E. W.; Lieber, C. M. *Science* **1996**, *272*, 523.
- (5) (a) Suarez, M. F.; Compton, R. G. *J. Electroanal. Chem.* **1999**, *462*, 211. (b) Hwang, B. J.; Santhanam, R.; Lin, Y.-L.; *J. Electrochem. Soc.* **2000**, *147*, 2252.
- (6) (a) Sadki, S.; Schottland, P.; Brodie, N.; Sabouraud, G. *Chem. Soc. Rev.* **2000**, *29*, 283. (b) Skotheim, T. A.; Elsenbaumer, R. L.; Reynolds, J. R. *Handbook of Conducting Polymers*; Marcel Dekker: New York, 1997; Vols. 1 and 2. (c) Nalwa, H. S. *Handbook of Organic Conductive Molecules and Polymers*; Wiley: Chichester, U.K., 1997; Vols. 1–4. (d) Park, S.-M. *Handbook of Organic Conductive Molecules and Polymers*; Nalwa, H. S., Ed.; Wiley: Chichester, U.K., 1997; Vol. 3.
- (7) (a) Huang, W.-S.; Humphrey, B. D.; MacDiamid, A. G. *J. Chem. Soc., Faraday Trans. 1* **1986**, *82*, 2385. (b) Stilwell, D. E.; Park, S.-M. *J. Electrochem. Soc.* **1988**, *135*, 2491. (c) Stilwell, D. E.; Park, S.-M. *J. Electrochem. Soc.* **1988**, *135*, 2497.
- (8) (a) Stilwell, D. E.; Park, S.-M. *J. Electrochem. Soc.* **1988**, *135*, 2254. (b) Hoier, S. N.; Park, S.-M. *J. Electrochem. Soc.* **1993**, *140*, 2454. (c) Kim, B. S.; Kim, W. H.; Hoier, S. N.; Park, S.-M. *Synth. Met.* **1995**, *69*, 455.
- (9) (a) Stilwell, D. E.; Park, S.-M. *J. Electrochem. Soc.* **1989**, *136*, 427. (b) Shim, Y. B.; Won, M.-S.; Park, S.-M. *J. Electrochem. Soc.* **1990**, *137*, 538. (c) Hoier, S. N.; Park, S.-M. *J. Phys. Chem.* **1992**, *96*, 5188.
- (10) (a) Choi, S.-J.; Park, S.-M. *J. Electrochem. Soc.* **2002**, *149*, E26. (b) Lee, J.-Y.; Park, S.-M. *J. Electrochem. Soc.* **2000**, *147*, 4189. (c) Ko, J. M.; Rhee, H. W.; Park, S.-M.; Kim, C. Y. *J. Electrochem. Soc.* **1990**, *137*, 905.
- (11) (a) Yang, R.; Smyrl, W. H.; Evans, D. F.; Hendrickson, W. A. *J. Phys. Chem.* **1992**, *96*, 1428. (b) Jeon, D.; Kim, J.; Gallagher, M. C.; Willis, R. F. *Science* **1992**, *256*, 1662. (c) Ho, P. K.; Zhang, P.-C.; Zhou, L.; Li, S. F. Y.; Chan, H. S. O. *Phys. Rev. B* **1997**, *56*, 15919.
- (12) (a) McCullough, R. D.; Williams, S. P. *J. Am. Chem. Soc.* **1993**, *115*, 11608. (b) Hao, Q.; Kulikov, V.; Mirsky, V. M. *Sens. Actuators B: Chem.* **2003**, *94*, 352.
- (13) Penner, R. M.; Van Dyke, L. S.; Martin, C. R. *J. Phys. Chem.* **1988**, *92*, 5274.
- (14) (a) www.molec.com (applications/imaging modes). (b) Kelley, T. W.; Granstrom, E. L.; Frisbie, C. D. *Adv. Mater.* **1999**, *11*, 261.
- (15) (a) Pyun, C.-H.; Park, S.-M. *Anal. Chem.* **1986**, *58*, 251. (b) Zhang, C.; Park, S.-M. *Anal. Chem.* **1988**, *60*, 1639. (c) Zhang, C.; Park, S.-M. *Bull. Korean Chem. Soc.* **1989**, *10*, 302.

- (16) (a) Diaz, A. F.; Hall, B. *IBM J. Resl. Develop.* **1983**, 27, 342. (b) Downward, A. J.; Pletcher, D. *J. Electroanal. Chem.* **1986**, 206, 139. (c) Zotti, G.; Shiavon, G.; Berlin, A.; Pagani, G. *Electrochim. Acta* **1989**, 34, 881. (d) Otero, T. F.; Rodriguez, J. *Synth. Met.* **1992**, 51, 307.
- (17) Otero, T. F.; Rodriguez, J. *J. Electroanal. Chem.* **1994**, 379, 513.
- (18) Semenikhin, O. A.; Jiang, L.; Iyoda, T.; Hashimoto, K.; Fujishima, A. *J. Phys. Chem.* **1996**, 100, 18603.
- (19) (a) Zotti, G.; Martina, S.; Wegner, G.; Schlüter, A.-D. *Adv. Mater.* **1992**, 4, 798. (b) John, R.; Wallace, G. G. *J. Electroanal. Chem.* **1991**, 306, 157.
- (20) (a) Stilwell, D. E.; Park, S.-M. *J. Electrochem. Soc.* **1989**, 136, 688. (b) Park, D.-S.; Shim, Y.-B.; Park, S.-M. *J. Electrochem. Soc.* **1993**, 140, 609. (c) Park, D.-S.; Shim, Y.-B.; Park, S.-M. *J. Electrochem. Soc.* **1993**, 140, 2749.
- (21) (a) Israelachvili, J. *Intermolecular and Surface Forces*; Academic Press: London, 1992. (b) Riedo, E.; Brune, H. *Appl. Phys. Lett.* **2003**, 83, 1986. (c) Han, D.-H.; Lee, H. J.; Park, S.-M. *Electrochim. Acta* **2005**, 50, 3085.
- (22) (a) Forrest, S. R. *Nature* **2004**, 428, 911. (b) the special issue on Organic Electronics *Chem. Mater.* **2004**, 16, 4381–4846.
- (23) (a) Pud, A. A. *Synth. Met.* **1994**, 66, 1. (b) Novak, P. *Electrochim. Acta* **1992**, 37, 1227.
- (24) (a) Toniolo, R.; Hummelgen, I. A. *Macromol. Mater. Eng.* **2004**, 289, 311. (b) Aziz, H.; Popovic, Z. D. *Chem. Mater.* **2004**, 16, 4522.
- (25) (a) Mecerreyes, D.; Alvaro, V.; Cantero, I.; Bengoetxea, M.; Calvo, P. A.; Grande, H.; Rodriguez, J.; Pomposo, J. A. *Adv. Mater.* **2002**, 14, 749. (b) Liu, Y.-C.; Hwang, B.-J. *J. Electroanal. Chem.* **2001**, 501, 100. (c) Kuhn, H. H.; Child, A. D.; Kimbrell, W. C. *Synth. Met.* **1995**, 71, 2139.